

High-Order Mimetic Finite Difference Methods on Nonuniform Grids

J. E. Castillo* J. M. Hyman† M. J. Shashkov† S. Steinberg‡

Abstract

By combining the support-operators method with the mapping method, we have derived new mimetic fourth-order accurate discretizations of the divergence, gradient, and Laplacian on nonuniform grids. These finite difference operators mimic the differential and integral identities satisfied by the differential operators. For example, the discrete divergence is the negative of the adjoint of the discrete gradient and consequently the Laplacian is a symmetric negative operator. We analyze the loss of accuracy in the approximations when the grid is rough and include numerical examples demonstrating the effectiveness of the higher order methods on nonuniform grids in one and two dimensions. The analysis and examples are for fourth-order finite difference methods, but the approach can be extended to create approximations of arbitrarily high order.

Key words: finite-difference, high-order, non-uniform grids, sensitivity, numerical analysis, partial differential equations.

AMS subject classifications: 65D25, 65G99, 65M06.

1 Introduction

The main goal of this research is to construct local high-order difference approximations of differential operators on nonuniform grids that mimic the symmetry properties of the continuum differential operators. Partial differential

equations (PDEs) solved with these mimetic difference approximations often automatically satisfy discrete versions of conservation laws and analogies to Stoke's theorem that are true in the continuum and, therefore, are more likely to produce physically faithful results. These symmetries are easily preserved by local discrete high-order approximations on uniform grids, but are difficult to retain in high-order approximations on nonuniform grids. We also desire the approximations to be local and use only function values at nearby points in the computational grid. These methods are especially efficient on computers with distributed memory.

We desire the methods to be high-order. The use of higher-order approximations reduces the number of points needed in the discretization and consequently reduces the computational cost to achieve a desired accuracy [9, 4]. This savings is inversely proportional to the number of grid points raised to the order of the method. Also, because the number of grid points in a calculation increases with the power of the dimension, the higher-order methods are extremely effective in higher dimensions. If, however, the higher-order approximations are less accurate or less stable than low order methods on rough grids, then all of the advantages may be lost.

A straight-forward method to construct high-order accurate approximations to the derivatives of a function defined on a nonuniform grid is to construct and differentiate a Lagrange interpolating polynomial [7]. On nonuniform grids, the difference approximations to the gradient operator **grad**, and the divergence operator, **div**, generated by Lagrange interpolation are rarely mimetic. Furthermore, their composition to form the Laplacian operator is often not negative definite.

If, however, the grid and function are first mapped to a uniform grid, the derivatives approximated there using Lagrange interpolation, and the results then mapped back to the original nonuniform grid, the resulting finite difference approximations can be shown to be mimetic, provided that at each step of the process the symmetry relationships are preserved. In expressing these discrete approximations, special care must be taken to preserve the symmetry rela-

*Department of Mathematics, SDSU, San Diego CA 92182, U.S.A.

†Los Alamos National Laboratory, Theoretical Division and Center for Nonlinear Science, MS-B284, Los Alamos, NM 87545, U.S.A.

‡Department of Mathematics University of New Mexico Albuquerque, NM 87131, U.S.A.

tionships between differential operators. It is these symmetry relationships that maintain the physical properties such as the conservation laws satisfied by a PDE in divergence form. In this paper, we derive an approach that preserves these relationships and guarantees that the resulting high-order approximations are mimetic.

The accuracy of the approximations depends as much upon the smoothness of the grid as the smoothness of the function being differentiated. Thus, a fourth-order approximation on smooth grids degenerates to lower order on rough grids. We analyze this loss of accuracy and verify that it occurs gracefully. We also verify that even on relatively rough grids, the fourth-order discretizations are computationally more efficient than the standard second-order discretization.

We first derive high-order mimetic approximations in one space dimension analogous to the divergence, defined at the nodes, and the gradient, defined in the cells. The discrete operators are required to be the negative adjoints of each other. The second derivative (Laplacian) is approximated by the composition of the first-order operators and consequently is a symmetric operator. This approach, based on the support-operator method [18, 19], guarantees that the resulting difference scheme preserves the symmetry properties. For example, the conservative property [13] for PDEs in divergence form is automatically preserved on nonuniform grids.

The construction and analysis of the higher-order schemes in 1D proceeds by first using Lagrange interpolation to construct higher-order approximations on a uniform grid and then using the mapping method [10, 20] to extend the approximation to nonuniform grids. The resulting approximation in 1D is then shown to be an example of a support-operator [18, 19] method, and consequently the scheme is mimetic. In 2D we also use the mapping method to construct the discrete analog of the divergence and directly use the support-operators method to construct finite-difference approximations for the gradient, and consequently in 2D these approximations are mimetic.

The accuracy of high-order approximations on nonuniform grids is sensitive to the smoothness of the grid. The importance of errors introduced into second-order difference schemes by nonuniform grids has been extensively studied [1, 3, 5, 6, 12, 14, 15, 16, 17, 21], but there has been little analysis or numerical comparisons for higher-order approximations on nonuniform grids [8, 9].

When generating a grid for a complex domain, it can be difficult to generate a smooth grid. Because of this, it is important to understand the impact of roughness in the grid on the quality of the approximations. In 1D we prove ana-

lytically, and confirm numerically, that the approximations we propose are fourth-order accurate on smooth grids and that the accuracy of the approximation decreases slowly as the smoothness of the grid decreases. The numerical verification is first done using an analytic transformation, with a jump in one of its derivatives, to map the grid. Next, we numerically study the accuracy of the difference approximations on a sequence of random perturbations of different order with respect to the uniform grid spacing. Numerical investigations of truncation errors and accuracy in 2D are in general similar to 1D, but truncation errors in 2D are much more sensitive to grid quality.

After defining the notation and basic ideas, we construct the higher-order mimetic approximations and analyze their errors and compare their accuracy and efficiency in numerical experiments.

2 Discretizations in 1D

The domain for the functions to be discretized, without loss of generality, can be chosen as the unit interval. This interval is divided into cells with endpoints called nodes. We denote functions defined at the nodes as *nodal functions*. These functions are analogous to vector functions, while *cell functions* are analogous to scalar functions defined at some point within the cells.

Consider the domain $[0, 1]$ and the irregular grid with nodes $\{x_i, i = 1, \dots, M\}$, with $x_i < x_{i+1}$. The size of the grid is measured by $\Delta x = \max_{1 \leq i \leq M-1} |x_{i+1} - x_i|$. In one dimension, discrete vector functions have one component, $\vec{W} = (WX, 0, 0)$, with values defined at the nodes $WX = \{WX_1, WX_2, \dots, WX_M\}$.

Within a cell with end points x_i and x_{i+1} , we introduce the point $\hat{x}_{i+1/2}$. On uniform grids, the point \hat{x} is the midpoint $\hat{x}_{i+1/2} = x_{i+1/2} \equiv (x_{i+1} + x_i)/2$ of the cell, and it is near the midpoint on nonuniform grids. The point $\hat{x}_{i+1/2}$ is the location where the discrete scalar function values $U = (U_{3/2}, \dots, U_{M-1/2})$, are defined. (An exact definition of $\hat{x}_{i+1/2}$ will be given later.)

2.1 The mapping method.

The mapping method [10, 20, 8] assumes that the grid is given by a mapping X ,

$$(1) \quad x_i = X(\xi_i), \quad i = 1, \dots, M;$$

where the ξ_i give a uniform grid, with mesh spacing $h = 1/(M-1)$ in the interval $[0, 1]$ which is called *logical space* (the grid is called the logical grid). The first derivative is

defined by

$$(2) \quad \frac{df}{dx} = \frac{df}{d\xi} \left(\frac{dx}{d\xi} \right)^{-1}.$$

This approach transforms the problem of approximating a derivative on a *nonuniform* grid to approximating two derivatives, $\frac{df}{d\xi}$ and $\frac{dx}{d\xi}$ on a *uniform* grid.

The same technique can be used to construct an approximation of the second derivative by using the chain rule

$$(3) \quad \frac{d^2u}{dx^2} = \left(\frac{d^2u}{d\xi^2} \frac{dx}{d\xi} - \frac{du}{d\xi} \frac{d^2x}{d\xi^2} \right) / \left(\frac{dx}{d\xi} \right)^3,$$

where all derivatives are approximated on a uniform grid, or it can be constructed as a composition of the discrete divergence **DIV** and gradient **GRAD** operators. The chain rule direct approach does not preserve many of the symmetry properties of the Laplacian, such as the divergence form, and is considerably more complicated in higher dimensions. Therefore we will only consider constructing the higher derivatives as a composition of the elementary operators **DIV** and **GRAD**.

The accuracy of the difference approximations constructed by the mapping method depends on both the continuity of the function defined on the grid and on the smoothness of the grid. In solving PDEs; often it is natural to require that the function being differentiated, $f(x)$, is smooth, but the grid may be prescribed by a process where we cannot assume that $X(\xi)$ is smooth. Consequently $\tilde{f}(\xi) = f(X(\xi))$ may not be smooth, even when f is well-behaved as a function of x . Therefore, estimates of the truncation error for high-order approximations must include an analysis based on both the smoothness of the function and the transformation.

If D_ξ approximates $d/d\xi$ on a uniform grid to $O(h^q)$, where $h = \xi_{i+1} - \xi_i$, then the approximation of D_x on a nonuniform grid

$$(4) \quad D_x f(x) = \frac{D_\xi \tilde{f}(\xi) + O(h^q)}{D_\xi X(\xi) + O(h^q)} = \frac{D_\xi \tilde{f}(\xi)}{D_\xi X(\xi)} + O(h^q)$$

$$\tilde{f}(\xi) = f(X(\xi))$$

is also $O(h^q)$.

If second-order central-differences are used to approximate the derivatives on the logical grid in (2) then the truncation error is, in general, first-order with respect to Δx , but if the transformation is smooth, then the truncation error is $O(h^2)$.

2.2 The support operators method

We introduce two discretizations for the first derivative based on the projections of the gradient and divergence

operators. In higher dimensions, the gradient **grad** operates on a scalar function to produce a vector function, while the divergence **div** operates on a vector function to produce a scalar function. In one dimension, a vector function $w = (w_x, 0, 0)$ has only one component and **div** is the derivative of this component. The **grad** is the usual derivative of a scalar function. We require the approximations to satisfy symmetry properties that come from an analogy to the higher-dimensional divergence, gradient, and Laplacian. In the continuum, the divergence and gradient are negative adjoints of each other, $\mathbf{div}^* = -\mathbf{grad}$, and the Laplacian is given by $\Delta = \mathbf{div grad}$. The adjointness requirement on the divergence and gradient implies that the Laplacian is a negative symmetric operator. One goal here is to construct high-order discrete analogs, **DIV** and **GRAD**, of the divergence and gradient so that $\mathbf{DIV}^* = -\mathbf{GRAD}$ and then use $\mathbf{LAP} = \mathbf{DIV GRAD}$ as an approximation of the second derivative. The approximations constructed are fourth-order, but the construction can be extended to create approximations of arbitrarily high order.

One of the most costly parts of many simulations is the inversion of the discrete Laplacian. Some of the most efficient methods for solving these equations require the discrete Laplacian to be a negative definite, symmetric operator. Mimetic discretizations of the Laplacian or, more generally, symmetric elliptic operators, automatically produce discrete operators that are symmetric and negative definite [18, 19].

The integral identity

In the support-operator method, the approximations of the divergence and gradient must satisfy a difference analog of integral identity

$$(5) \quad \int_V u \mathbf{div} \vec{w} dV + \int_V (\vec{w}, \mathbf{grad} u) dV = \oint u (\vec{w}, \vec{n}) dS.$$

This identity can also be written in terms of inner products,

$$(6) \quad (f, g)_H = \int_V f g dV, \quad (\vec{a}, \vec{b})_{\mathcal{H}} = \int_V (\vec{a}, \vec{b}) dV.$$

For functions which are equal to zero on the boundary, the integral identity (5) is

$$(7) \quad (u, \mathbf{div} \vec{w})_H + (\mathbf{grad} u, \vec{w})_{\mathcal{H}} = 0,$$

that is, differential operators **div** and **grad** are negative adjoints of each other:

$$(8) \quad \mathbf{grad} = -\mathbf{div}^*.$$

A discrete analog of the adjoint relationship (8) can be found by introducing the following inner products in spaces of discrete functions:

$$(9) \quad (F, G)_{H_h} = \sum_i F_{i+1/2} G_{i+1/2} VC_{i+1/2}$$

and

$$(10) \quad (\vec{A}, \vec{B})_{\mathcal{K}_h} = \sum_i AX_i BX_i VN_i,$$

where the volumes of the cell $VC_{i+1/2}$ and the volumes of the nodes VN_i depend upon the mapping and must be defined consistently for each of the numerical methods.

If the discrete functions are zero near the boundary, then we will define the operator **GRAD** from the following discrete identity

$$\sum_i U_{i+1/2} (\mathbf{DIV} \vec{W})_{i+1/2} VC_{i+1/2} + \sum_i WX_i (\mathbf{GRAD} U)_i VN_i = 0,$$

or

$$(11) \quad (U, \mathbf{DIV} \vec{W})_{H_h} + (\mathbf{GRAD} U, \vec{W})_{\mathcal{K}_h} = 0,$$

and, consequently, the discrete operators are also negative adjoints of each other:

$$(12) \quad \mathbf{GRAD} = -\mathbf{DIV}^*.$$

2.3 Difference approximations

The error estimate for the Lagrange interpolant of order n (using $n + 1$ points) for a smooth function f is

$$(13) \quad |f(x) - L_n(x)| \leq \frac{\max_{\tilde{x}}(f^{n+1}(\tilde{x}))}{(n+1)!} R(\Delta x)^{n+1},$$

and

$$(14) \quad \frac{df}{dx}(x) = \frac{dL_n}{dx}(x) + O((\Delta x)^n),$$

where \tilde{x} is a point in the interpolation interval, and R is some constant which depends on the interpolation points and scales as h^n . Thus L_3 gives a third-order approximation for the first derivative on nonuniform grids. On uniform grids fortunate error cancelation makes this approximation fourth-order at the midpoint of the center cell, and formula for approximation of first derivative becomes

$$(15) \quad (D_x f)_{i+1/2} = \frac{-f_{i+2} + 27 f_{i+1} - 27 f_i + f_{i-1}}{24 \Delta x}.$$

The analogous sixth-order formula is

$$(16) \quad (D_x f)_{i+1/2} = \frac{\{-9 f_{i-2} + 125 f_{i-1} - 2250 f_i + 2250 f_{i+1} - 125 f_{i+2} + 9 f_{i+3}\}}{(1920 \Delta x)}.$$

To maintain the analogy that vector functions are defined on the nodes and scalar functions are defined on cells, the discrete divergence **DIV** maps nodal functions to cell functions and the discrete gradient, **GRAD** operator maps cell functions to nodal functions. The two simplest natural approximations of these operators are

$$(17) \quad (\mathbf{DIV} \vec{W})_{i+1/2} = \frac{\vec{W}_{i+1} - \vec{W}_i}{x_{i+1} - x_i},$$

and

$$(18) \quad (\mathbf{GRAD} U)_i = \frac{U_{i+1/2} - U_{i-1/2}}{\hat{x}_{i+1/2} - \hat{x}_{i-1/2}}.$$

The first formula is second order approximation on any grid, and second formula is first order on non-smooth grid and second order on smooth grids.

High order discrete divergence operator DIV
On a uniform grid (15) gives

$$(19) \quad (\mathbf{DIV} \vec{W})_{i+1/2} = \frac{-WX_{i+2} + 27WX_{i+1} - 27WX_i + WX_{i-1}}{24VC_{i+1/2}},$$

with the cell volume, $VC_{i+1/2} = h$, a fourth-order approximation for the divergence at $\xi_{i+1/2} = (\xi_i + \xi_{i+1})/2$.

On a nonuniform grid, using this formula in (2) for smooth functions and transformations, the mapping method approximation for the divergence with the cell volume

$$(20) \quad VC_{i+1/2} = \frac{(-x_{i+2} + 27x_{i+1} - 27x_i + x_{i-1})}{24},$$

is $O(h^4)$ accurate at the image of $\xi_{i+1/2}$, $\hat{x}_{i+1/2} = X(\xi_{i+1/2})$. Usually $\hat{x}_{i+1/2} \neq x_{i+1/2} \equiv (x_i + x_{i+1})/2$. Because the difference between $\hat{x}_{i+1/2}$ and $x_{i+1/2}$ is $O(\Delta x^2)$, this distinction only plays a role for high-order methods. In our truncation error analysis we are careful to ensure that the *mid-point projection* is the image under the transformation of the mid-point in *logical space* and not the center point of the central interval. If the function $X(\xi)$ is not known explicitly, then this point can be approximated by Lagrange interpolation to fourth-order by

$$(21) \quad \hat{x}_{i+1/2} \approx (-x_{i+2} + 9x_{i+1} + 9x_i - x_{i-1})/16.$$

On rough grids, the denominator $VC_{i+1/2}$, given by (20) can vanish. That is, even though X is a one-to-one mapping, the numerical approximation of the map may not be, causing the difference approximation to fail. Luckily, this only occurs on very rough grids.

The volume VC (and VN) must be positive to ensure that the expressions (2.2) (10) satisfy the axioms of an inner product. To illustrate how this failure can occur, consider the function $u_i = 1$ for $i = i_0$ and $u_i = 0$ for all other i , then

$$(22) \quad (u, u)_{H_h} = VC_{i_0+1/2},$$

which must be positive. When a volume VC is zero or negative the length of a nonzero vector is zero or negative, and the expression given in (2.2) does not satisfy the axioms of an inner product. Similar results hold for the inner product of discrete vectors. This can produce some non-physical consequences. For example, some quantity which is always positive in the physical model, such as energy, can be zero or negative. Thus, to use the mapping method for some given grid, one must check that VC and VN are always positive.

High order discrete gradient operator **GRAD**

The formula (15), translated by $1/2$,

$$(\mathbf{GRAD} U)_i = \frac{-U_{i+3/2} + 27 U_{i+1/2} - 27 U_{i-1/2} + U_{i-3/2}}{24 V N_i}$$

with the nodal volume, $V N_i = h$, is a fourth-order approximation for the gradient on a uniform grid.

On a nonuniform grid, using

$$V.N_i = \frac{-\hat{x}_{i+3/2} + 27 \hat{x}_{i+1/2} - 27 \hat{x}_{i-1/2} + \hat{x}_{i-3/2}}{24}$$

provides a fourth-order approximation at the image $X(\xi_i)$, that is at x_i .

3 Truncation error analysis

We define the truncation error as the difference between the projection to a grid point of the derivative of a smooth function and the discrete difference approximation of the derivative using values of the smooth function projected to the grid points. The *cell projection* operator, p_h , maps a smooth scalar function to discrete cell-valued functions:

$$(1) \quad (p_h u)_{i+1/2} = u_{i+1/2} \equiv u(\hat{x}_{i+1/2}).$$

The *nodal projection* operator, P_h , maps a smooth vector function to its values at the nodes

$$(2) \quad (P_h \vec{w})_i = \vec{w}_i \equiv \vec{w}(x_i).$$

If \vec{w} is a smooth vector function, then the truncation error of the discrete divergence $\psi_{\mathbf{DIV}}$ is the nodal function

$$(3) \quad \psi_{\mathbf{DIV}} \vec{w} = p_h \left(\frac{d\vec{w}}{dx} \right) - \mathbf{DIV} (P_h \vec{w}).$$

If u is a smooth scalar function, the truncation error of the discrete gradient $\psi_{\mathbf{GRAD}}$ is

$$(4) \quad \psi_{\mathbf{GRAD}} u = \mathbf{GRAD}(p_h u) - P_h \left(\frac{du}{dx} \right).$$

The approximations (17) and (18) are second order on uniform grids, but the approximation to the gradient is only first order on nonuniform grids. One goal of this paper is to derive higher-order analogs of these discrete operators.

The accuracy of the discrete divergence, gradient and Laplacian operators depend upon the smoothness of the grid transformation. In this section, we present results of the truncation errors analysis for **DIV**, **GRAD** and **LAP** (details can be found in [2]) on grids generated by an analytic transformation with different levels of differentiability, and on randomly generated grids. We describe the analytic grid transformation as C^k when the first k derivatives of the map are continuous. (In our examples, the $k+1$ derivative has a jump discontinuity). For our random grid examples, the identity map is perturbed by a random multiple of h^k .

If f is a C^{k-1} function and the k -th derivative is bounded, then

$$(5) \quad f(x+h) = \sum_{j=0}^{k-1} \frac{f^{(j)}(x) h^j}{j!} + \frac{F_k h^k}{k!},$$

where F_k is some average value of $f^{(k)}$. For a C^0 mapping with bounded derivative, by Taylor series expansion about the point x_i , we can express

$$(6) \quad x_{i\pm k} = x_i \pm k h C_{i\pm k},$$

where $C_{i\pm k}$ are bounded by the first derivative of X .

For a C^1 mapping with bounded second derivative, we have

$$(7) \quad x_{i\pm k} = x_i \pm k h \left(\frac{dX}{d\xi} \right)_i + \frac{k^2}{2} h^2 C_{i\pm k}$$

where $C_{i\pm k}$ are bounded by the second derivative of X .

DIV and **GRAD** error analysis

The truncation error for the fourth order operator **DIV**, operating on a smooth function $\vec{w}(x)$, is obtained by Taylor series about $\hat{x}_{i+1/2}$. The image of the midpoint in logical space plays a critical role in our analysis. Because, in general, the mapping is not known explicitly, it is important to accurately approximate this image in analyzing the truncation error of the fourth-order methods. We use the definition (21) for $\hat{x}_{i+1/2}$.

For a C^0 mapping $\psi_{\mathbf{DIV}}$ are order h . The same result is obtained for $\psi_{\mathbf{GRAD}}$. For a C^1 mapping (7), $\psi_{\mathbf{DIV}}$ is order h^3 , but truncation error for **GRAD** is only order h^2 .

Mapping	GRAD	DIV	LAP
C^0	1	1	0
C^1	2	3	1
C^2	3	4	2
C^3	4	4	3
C^4	4	4	4

Table 1: Theoretical estimates for the order of approximation of the fourth-order discrete operators, analyzed in section 3, as a function of the smoothness of the map.

These results can be extended to non-smooth grids. We define the $O(h^k)$ random grid by

$$(8) \quad x_i = \xi_i + h^k R_i,$$

where the R_i 's are random numbers uniformly distributed in $[-1/4, 1/4]$.

On order h random grids both ψ_{DIV} , ψ_{GRAD} are order h . For order h^2 random grid ψ_{DIV} is third-order, but similar to case of C^1 mapping ψ_{GRAD} is only second-order.

The cases for higher-order smoothness of the analytical grid and high order random perturbation of the uniform grid, are handled similarly, and results are summarized in Table 1.

LAP error analysis

Because $\text{DIV} = -\text{GRAD}^*$, the Laplacian, $\text{LAP} = \text{DIV GRAD}$, is symmetric and negative (but may not be negative definite). We now estimate its truncation error in terms of the truncation errors for the divergence and gradient.

For a uniform grid, the superposition of DIV and GRAD is

$$(\text{LAP } U)_{i+1/2} = \frac{1}{576 h^2} (U_{i+7/2} - 54 U_{i+5/2} + 783 U_{i+3/2} - 1460 U_{i+1/2} + 783 U_{i-1/2} - 54 U_{i-3/2} + U_{i-5/2}).$$

On a nonuniform grid, the explicit formula for the high order LAP operator is extremely complex. In practice, e.g. when programming the operator on the computer, we define the Laplacian on nonuniform grids as a composition of the discrete DIV and GRAD operators.

Combining (3) and (4),

$$(9) \quad \psi_{\text{DIV GRAD}} u = \psi_{\text{DIV}}(\text{grad } u) - \text{DIV } \psi_{\text{GRAD}}(u).$$

The truncation error of the first term on the right side of this equation is the same as for DIV , but the truncation error for the second term is one order less than for the GRAD . Because this truncation error was estimated by using the estimates for the individual operators independently, there may be some undetected cancellation and the truncation error may be less than these estimates. However, the numerical results for random grids confirm that the estimates are, in fact, optimal. Similar results can be obtained for the operator grad div and its approximation GRAD DIV .

Although the truncation error for the Laplacian may reduce to $O(1)$ on rough grids, the convergence rate for the solutions of elliptic boundary value problems and parabolic diffusion equations remains at least second order in all the numerical experiments we performed with the methods. This has been proved for similar methods in [11].

In summary, on the rough grids the truncation error for LAP is one order less than that of GRAD , and, for smooth enough grids (C^1 , C^2), the truncation error for DIV is one order higher than the truncation error for GRAD , for very smooth grid (C^3 and higher) for both operator truncation error is fourth order.

4 Discretizations in 2D

4.1 The mapping method

In 2D we also need to approximate the operators div and grad . The derivation of a discrete approximation of derivatives using the mapping method approach begins by assuming that there is a transformation

$$(1) \quad \begin{aligned} x &= X(\xi, \eta), & y &= Y(\xi, \eta), \\ 0 &\leq \xi \leq 1, & 0 &\leq \eta \leq 1, \end{aligned}$$

between the physical region and a unit square in logical space. Given such a transformation and two positive integers, M and N , set $\Delta\xi = 1/M$ and $\Delta\eta = 1/N$. The points $(x_{i,j}, y_{i,j})$ given by

$$\begin{aligned} x_{i,j} &= x(i \Delta\xi, j \Delta\eta), & y_{i,j} &= y(i \Delta\xi, j \Delta\eta), \\ 0 &\leq i \leq M, & 0 &\leq j \leq N, \end{aligned}$$

form a grid on the physical region.

The first and second derivatives of a function can be expressed directly as a function of the derivatives on a regular reference grid and the mesh metrics of the map from the physical (x, y) grid to the reference (ξ, η) grid. Using this straight-forward definition we have

$$\begin{bmatrix} u_x \\ u_y \\ u_{xx} \\ u_{xy} \\ u_{yy} \end{bmatrix} = \begin{bmatrix} \xi_x & \eta_x & 0 & 0 & 0 \\ \xi_y & \eta_y & 0 & 0 & 0 \\ \xi_{xx} & \eta_{xx} & \xi_x^2 & 2\xi_x\eta_x & \eta_x^2 \\ \xi_{xy} & \eta_{xy} & \xi_x\xi_y & \xi_x\eta_y + \xi_y\eta_x & \eta_x\eta_y \\ \xi_{yy} & \eta_{yy} & \xi_y^2 & 2\xi_y\eta_y & \eta_y^2 \end{bmatrix} \begin{bmatrix} u_\xi \\ u_\eta \\ u_{\xi\xi} \\ u_{\xi\eta} \\ u_{\eta\eta} \end{bmatrix}$$

where

$$(\)_\xi = \frac{\partial}{\partial \xi}, \quad (\)_\eta = \frac{\partial}{\partial \eta}.$$

If the derivatives of the map are not known explicitly, then they too must be expressed in terms of derivatives on the uniform reference grid.

Using the Jacobian, J , of the map and its derivatives,

$$J = x_\xi y_\eta - x_\eta y_\xi,$$

$$J_\xi = x_{\xi\xi} y_\eta + x_\xi y_{\xi\eta} - x_{\xi\eta} y_\xi - x_\eta y_{\xi\xi},$$

and

$$J_\eta = x_{\xi\eta} y_\eta + x_\xi y_{\eta\eta} - x_{\eta\eta} y_\xi - x_\eta y_{\eta\xi},$$

the mesh metrics can be expressed as derivatives on the (ξ, η) reference grid.

$$\xi_x = y_\eta/J, \quad \xi_y = -x_\eta/J, \quad \eta_x = -y_\xi/J, \quad \eta_y = x_\xi/J$$

$$\xi_{xx} = (-J_\xi y_\eta^2 + J y_\eta y_{\xi\eta} + J_\eta y_\xi y_\eta - J y_\xi y_{\eta\eta})/J^3,$$

$$\xi_{xy} = (J_\xi x_\eta y_\eta - J x_{\xi\eta} y_\eta - J_\eta x_\eta y_\xi + J x_{\eta\eta} y_\xi)/J^3,$$

(2)

$$\xi_{yy} = (-J_\xi x_\eta^2 + J x_\eta x_{\xi\eta} + J_\eta x_\xi x_\eta - J x_\xi x_{\eta\eta})/J^3,$$

$$\eta_{xx} = (-J_\eta y_\xi^2 + J y_\xi y_{\xi\eta} + J_\xi y_\xi y_\eta - J y_\xi y_{\eta\eta})/J^3,$$

$$\eta_{xy} = (J_\eta x_\xi y_\xi - J x_{\xi\eta} y_\xi - J_\xi x_\xi y_\eta + J x_{\xi\xi} y_\eta)/J^3,$$

and

$$\eta_{yy} = (-J_\eta x_\xi^2 + J x_\xi x_{\xi\eta} + J_\xi x_\xi x_\eta - J x_{\xi\xi} x_\eta)/J^3.$$

The derivative approximations generated by this approach can be combined to give accurate approximations for the **GRAD**, **DIV** and **LAP** on a smooth grid, but the resulting approximations, in addition to being extremely

complicated, will not be mimetic. Instead, we again use a combination of the mapping method and the method of support-operators to generate high order mimetic finite difference approximations for the **GRAD** and **DIV**. These can then be composed to approximate the Laplacian.

The formulas for the operators **DIV** and **GRAD** still contain derivatives of transformation and Jacobian at different points. If we know mapping analytically we can evaluate derivatives explicitly. The grids may be generated numerically (see, for example, [10]), or obtained from another calculations, such as occurs in Lagrangian fluid dynamics. For these cases we know only the coordinates of nodes: $x_{i,j}, y_{i,j}$. That is values of the functions $X(\xi, \eta), Y(\xi, \eta)$ at the nodes ξ_i, η_j . The derivatives of the transformation can be defined using finite-difference approximations of (2). These approximations should be at least the same order accuracy as the **GRAD** and **DIV** operators.

4.2 The support-operators method

For a discrete description of the vector field we will use Cartesian coordinates, $\vec{A} = (AX, AY)$. Therefore, differential operator divergence is

$$(3) \quad \text{div } \vec{A} = \frac{\partial AX}{\partial x} + \frac{\partial AY}{\partial y}.$$

Because the operator **div** is in divergence form, its approximation is constructed on the basis of the *conservative* or *symmetric form* of the transformed derivatives (see, for example, [10]),

$$\frac{\partial u}{\partial x} = \left\{ (u y_\eta)_\xi - (u y_\xi)_\eta \right\} / J$$

and

$$\frac{\partial u}{\partial y} = \left\{ (u x_\xi)_\eta - (u x_\eta)_\xi \right\} / J.$$

Therefore, for derivatives which form a divergence, we get

$$(4) \quad \frac{\partial AX}{\partial x} = \left\{ (AX y_\eta)_\xi - (AX y_\xi)_\eta \right\} / J$$

and

$$(5) \quad \frac{\partial AY}{\partial y} = \left\{ (AY x_\xi)_\eta - (AY x_\eta)_\xi \right\} / J.$$

Therefore, the problem of approximation of the operator **div** is reduced to approximation of the first derivatives of AX, AY and x, y with respect to logical variables ξ, η on a square grid.

Because we want to find an approximation for the operator **grad**, which preserves adjointness to the operator **div** in the discrete case, we consider how the main integral identity (5) works in the differential case. For the

first integral we have the following expression in terms of coordinates ξ, η :

$$(6) \quad \int_V u \mathbf{div} \vec{A} dV = \frac{1}{J} \left\{ \left[(AX y_\eta)_\xi - (AX y_\xi)_\eta \right] \left[(AY x_\xi)_\eta - (AY x_\eta)_\xi \right] \right\} d\xi d\eta.$$

To understand the expression for components $GX = \partial u / \partial x$ and $GY = \partial u / \partial y$ of the vector $\mathbf{grad} u$, obtained by using the integral identity, we write the following expression for the second integral

$$(7) \quad \int_V (\vec{A}, \mathbf{grad} u) dV = \int_V (AX \cdot GX + AY \cdot GY) J d\xi d\eta.$$

Integrating by parts in (6) and comparing terms near AX and AY in the transformed (6) and (7) we can conclude that

$$(8) \quad GX = \frac{\partial u}{\partial x} = (\tilde{u}_\xi y_\eta - \tilde{u}_\eta y_\xi) / J$$

and

$$(9) \quad GY = \frac{\partial u}{\partial y} = (\tilde{u}_\eta x_\xi - \tilde{u}_\xi x_\eta) / J.$$

4.3 Difference approximations

In the discrete case, to construct discrete analogs of \mathbf{div} and \mathbf{grad} we use a combination of the mapping and the support-operators method. Using the mapping method we approximate the operator \mathbf{div} based on the formulas (4), (5). We then use the support-operators method and the integral identity to obtain the expression for the discrete \mathbf{grad} , analogous to the formulas (8), (9). The approximations of the derivatives for \mathbf{div} and \mathbf{grad} can not be chosen independently; the approximation for \mathbf{grad} follows from the approximation for \mathbf{div} and the integral identity. This procedure allows us to keep adjointness of discrete operators similar to the differential case.

Therefore, the problem of constructing finite-difference operators \mathbf{DIV} and \mathbf{GRAD} in 2D is reduced to construction of some set of one dimensional operators, which will be analogs of the derivative in ξ and η directions, and projection operators to project values of functions in one location to another (for example projections from the centers of the edges to center of the cell and so on).

We also require that the finite-difference approximations on rectangular grids coincide with the one dimensional approximations considered in the first part of this paper.

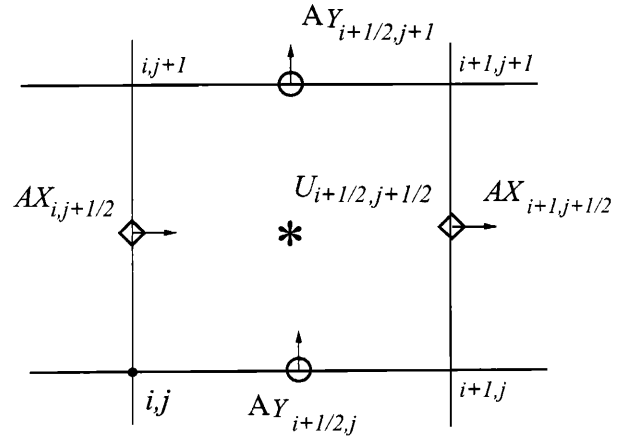


Figure 1: The stencil for the discretizations.

Spaces of discrete functions

To describe vector $\vec{A} = (AX, AY)$, we introduce the discrete spaces: space $H\xi$, which we use for description of component AX of the vector \vec{A} , is described by values on the middle of the edge $(i, j) - (i, j+1)$ in logical coordinates, that is, in point

$$(\xi_i, 0.5(\eta_{i,j} + \eta_{i,j+1})).$$

And space $H\eta$, which we use for description of component AY , is described by values in the middle of the edge $(i, j) - (i+1, j)$ in logical coordinates; That is, in point

$$(\xi_i, 0.5(\eta_{i,j} + \eta_{i,j+1})).$$

Therefore, discretization of the vector field is

$$\vec{A} = (AX, AY); \quad AX \in H\xi, \quad AY \in H\eta.$$

For description of scalar functions we use space HC , which is described by values of the scalar in the middle of the cell in logical coordinates, that is, in point

$$(0.5(\xi_i + \xi_{i+1}), 0.5(\eta_{i,j} + \eta_{i,j+1})).$$

Therefore discretization of scalars is $U \in HC$. Discretizations for vector and scalar functions are shown on figure 1.

Such discretization will be consistent with one dimensional considerations, because space $H\xi$ corresponds to a nodal discretization for the 1D (dependent only on x) case, and space HC corresponds to cell-centered discretization.

Operators D_ξ and D_ξ^*

To obtain fourth order approximations for \mathbf{div} and \mathbf{grad} on smooth grids we use one dimensional analogs of derivatives and projection operators. Again we need two analogs

of the first derivative $\partial/\partial\xi$:

$$\begin{aligned} D_\xi &: H\xi \rightarrow HC, \\ D_\xi^* &: HC \rightarrow H\xi. \end{aligned}$$

The expressions for these operators follow from one dimensional considerations:

$$\begin{aligned} (D_\xi A\xi)_{i+1/2,j+1/2} = \\ \{ -A\xi_{i+2,j+1/2} + 27 A\xi_{i+1,j+1/2} \\ - 27 A\xi_{i,j+1/2} + A\xi_{i-1,j+1/2} \} / (24h). \end{aligned}$$

$$\begin{aligned} (D_\xi^* U)_{i,j+1/2} = \\ \{ -U_{i+3/2,j+1/2} + 27 U_{i+1/2,j+1/2} \\ - 27 U_{i-1/2,j+1/2} + U_{i-3/2,j+1/2} \} / (24h). \end{aligned}$$

Similarly, we introduce differentiation operators D_η and D_η^* :

$$D_\eta : H\eta \rightarrow HC; \quad D_\eta^* : HC \rightarrow H\eta.$$

We also define projection operators,

$$P_\xi : H\xi \rightarrow HC; \quad P_\xi^* : HC \rightarrow H\xi.$$

with the same stencils as D_ξ and D_ξ^* . Formulas for the projection operators are similar to 1D formulas such (21).

$$\begin{aligned} (P_\xi A\xi)_{i+1/2,j+1/2} = \\ \{ -A\xi_{i+2,j+1/2} + 9 A\xi_{i+1,j+1/2} \\ + 9 A\xi_{i,j+1/2} - A\xi_{i-1,j+1/2} \} / 16, \end{aligned}$$

The definitions for operators P_η and P_η^* are similar.

If we use sixth or higher order approximations of the one dimensional operators, then we obtain approximations of correspondent order for **div** and **grad** on smooth grids. It is important to note that the form of **DIV** and **GRAD** operators are the same. For example, the sixth order formula for the operator D_ξ can be obtained from Lagrange interpolation and has the following form:

$$\begin{aligned} (D_\xi A\xi)_{i+1/2,j+1/2} = \frac{1}{1920h} \cdot \\ \{ -9 A\xi_{i-2,j+1/2} + 125 A\xi_{i-1,j+1/2} - 2250 A\xi_{i,j+1/2} + \\ - 2250 A\xi_{i+1,j+1/2} - 125 A\xi_{i+2,j+1/2} + 9 A\xi_{i+3,j+1/2} \}. \end{aligned}$$

This is convenient for programming, because if one decides to change from a scheme of one order to another, one only need change the formulas for one-dimensional operators.

Discrete operator DIV

If we know the transformation and its derivatives, then the operator **div** can be approximated by

$$\frac{\partial AX}{\partial x} \Big|_{\substack{\hat{x}_{i+1/2,j+1/2} \\ \hat{y}_{i+1/2,j+1/2}}} \approx (D_x AX)_{i+1/2,j+1/2} = \tag{10}$$

$$\begin{aligned} \frac{1}{J_{i+1/2,j+1/2}} \{ [D_\xi (AX y_\eta)]_{i+1/2,j+1/2} - \\ [D_\eta ((P_\eta^*(P_\xi AX)) y_\xi)]_{i+1/2,j+1/2} \}, \\ \frac{\partial AY}{\partial y} \Big|_{\substack{\hat{x}_{i+1/2,j+1/2} \\ \hat{y}_{i+1/2,j+1/2}}} \approx (D_y AY)_{i+1/2,j+1/2} = \tag{11} \end{aligned}$$

$$\begin{aligned} \frac{1}{J_{i+1/2,j+1/2}} \{ [D_\eta (AY x_\xi)]_{i+1/2,j+1/2} - \\ [D_\xi ((P_\xi^*(P_\eta AY)) x_\eta)]_{i+1/2,j+1/2} \}, \end{aligned}$$

where

$$\hat{x}_{i+1/2,j+1/2} = X(\xi_{i+1/2,j+1/2}, \eta_{i+1/2,j+1/2})$$

and

$$\hat{y}_{i+1/2,j+1/2} = Y(\xi_{i+1/2,j+1/2}, \eta_{i+1/2,j+1/2}).$$

Stencil for AX and AY for fourth order **DIV** operator is shown in figure 2.

Discrete operator GRAD

To obtain the **GRAD** operator we use a discrete analog of the integral identity. The first integral can be approximated as follows

$$\begin{aligned} (12) \quad \int_V u \operatorname{div} \vec{A} dV \approx \\ \sum_{i,j} U_{i+1/2,j+1/2} \{ \{ [D_\xi (AX y_\eta)]_{i+1/2,j+1/2} - \\ [D_\eta (P_\eta^*(P_\xi AX)) y_\xi]_{i+1/2,j+1/2} \} + \\ \{ [D_\eta (AY x_\xi)]_{i+1/2,j+1/2} - \\ [D_\xi (P_\xi^*(P_\eta AY)) x_\eta]_{i+1/2,j+1/2} \} \} h^2 \end{aligned}$$

Because we are trying to approximate the Cartesian components of the operator **grad**, the approximation for the second integral can be written as

$$\begin{aligned} (13) \quad \int_V (\vec{A}, \operatorname{grad} u) dV \approx \\ \sum_{i,j} 0.5 (AX_{i,j+1/2} GX_{i,j+1/2} + \end{aligned}$$

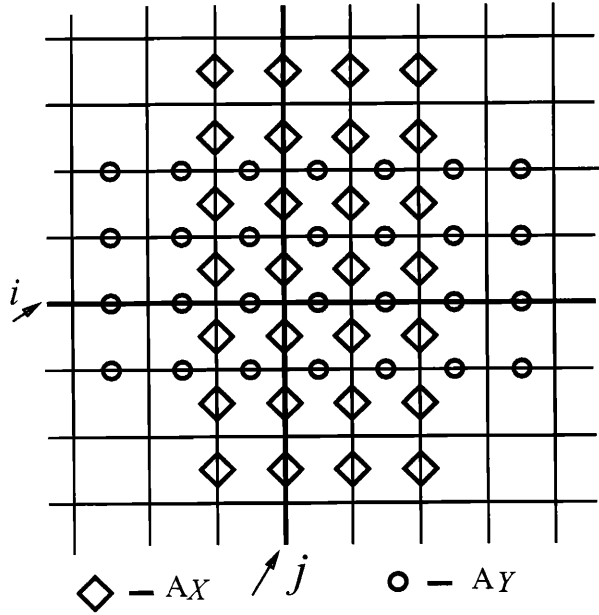


Figure 2: The stencil for AX and AY in the fourth order **DIV**.

$$\begin{aligned}
 & AX_{i+1,j+1/2} GX_{i+1,j+1/2} + \\
 & AX_{i+1/2,j} GX_{i+1/2,j} + \\
 & AX_{i+1/2,j+1} GX_{i+1/2,j+1}) VC_{i+1/2,j+1/2},
 \end{aligned}$$

where $VC_{i+1/2,j+1/2}$ is the volume of the cell.

A more general formula follows from the fact that

$$\int_V (\vec{A}, \mathbf{grad} u) dV = \int_V (AX GX + AY GY) dV$$

and the chosen type of discretization where AX relates to sides $(i, j) - (i, j + 1)$; and AY relates to sides $(i, j) - (i + 1, j)$.

The general formula is

$$\begin{aligned}
 (14) \quad & \int_V (\vec{A}, \mathbf{grad} u) dV \approx \\
 & \sum_{i,j} AX_{i,j+1/2} GX_{i,j+1/2} VX_{i,j+1/2} + \\
 & \sum_{i,j} AY_{i+1/2,j} GX_{i+1/2,j} VY_{i+1/2,j}
 \end{aligned}$$

where

$$\sum_{i,j} VX_{i,j+1/2} = V, \quad \sum_{i,j} VY_{i+1/2,j} = V.$$

Formula (13) follows from the general formula if we choose

$$VX_{i,j+1/2} = \frac{VC_{i+1/2,j+1/2} + VC_{i-1/2,j+1/2}}{2}$$

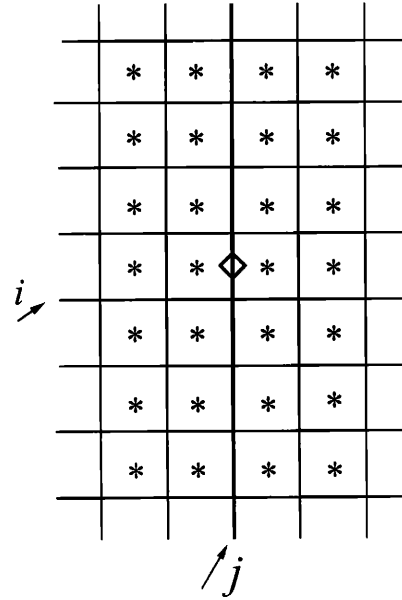


Figure 3: The stencil for the GX component of the fourth order **GRAD**.

and

$$VX_{i+1/2,j} = \frac{VC_{i+1/2,j+1/2} + VC_{i+1/2,j-1/2}}{2}.$$

If we know the transformation $X(\xi, \eta), Y(\xi, \eta)$ explicitly, we can use the following formulas:

$$\begin{aligned}
 VX_{i,j+1/2} &= J_{i,j+1/2} h^2 \\
 VY_{i+1/2,j} &= J_{i+1/2,j} h^2.
 \end{aligned}$$

For the last choice of VX, VY we get

$$\begin{aligned}
 (15) \quad & GX_{i,j+1/2} = \\
 & -\frac{1}{J_{i,j+1/2}} \left\{ [D_\xi^* U]_{i,j+1/2} y_\eta - \right. \\
 & \left. [P_\xi^* (P_\eta(y_\xi D_\eta^*(U)))]_{i,j+1/2} \right\} \\
 & GY_{i+1/2,j} = \\
 & -\frac{1}{J_{i+1/2,j}} \left\{ [D_\eta^* U]_{i+1/2,j} x_\xi - \right. \\
 & \left. [P_\eta^* (P_\xi(x_\eta D_\xi^*(U)))]_{i+1/2,j} \right\}.
 \end{aligned}$$

The stencil for GX is shown in figure 3. The stencil for GY is similar, we just need to turn the previous stencil 90 degrees.

5 Numerical experiments

We first verify the order of the truncation error estimates by numerical experiments on the grids described in the previous section. We then solve the time-dependent heat equation to determine the convergence rate of the fourth-order spatial discretization, combined with a high-order time discretization.

We show that the convergence rate for the maximum and mean-square norms are the same. We also confirm that the second-order method has a second-order convergence rate for all grids and that the fourth-order method has at least a second-order convergence for all grids. However, as the smoothness of the grid increases, so does the order of convergence for the fourth-order method. We finally demonstrate that on smooth nonuniform grids the fourth-order method is computationally more efficient than the second-order method for a prescribed accuracy. Furthermore the fourth-order method gives more accurate results when both use the same computational effort, even on rough grids.

5.1 Numerical investigation of truncation errors

The first examples are based on the analytic map

$$(1) \quad X(\xi) = \begin{cases} \frac{\xi}{d}, & 0 \leq \xi \leq r, \\ \frac{\xi}{d} + \frac{1}{d} \sum_{j=1}^k \frac{b_j \cdot (\xi - r)^j}{j!}, & r \leq \xi \leq 1, \end{cases}$$

where

$$d = 1 + \sum_{j=1}^k \frac{b_j \cdot (1 - r)^j}{j!}$$

is introduced for normalizing the mapping. The number of terms in the sum, k , is a parameter. This function produces a family of mappings with varying smoothness at the $\xi = r$. The C^0 grid is defined by setting $b_i = 1$ for $1 \leq i \leq k$. The C^1 mapping is defined by setting $b_1 = 0$ and $b_i = 1$ for $i > 1$. Smoother mappings are defined similarly.

Next we construct rough grids using random perturbations of a uniform grid. We define the $O(h^k)$ grid by

$$x_i = \xi_i + h^k R_i,$$

where the R_i 's are random numbers uniformly distributed in $[-1/4, 1/4]$.

The asymptotic truncation error E_h on a grid of M nodes, $h = 1/(M - 1)$, is estimated by

$$(2) \quad E_h = c h^q + O(h^{q+1}),$$

where q is the order of the error, and the constant c , the convergence-rate constant, is independent of M .

In the numerical examples the truncation errors were evaluated on a sequence of grids $h = 2^{-r}$ and the convergence rates estimated from the ratio between the norms of the errors (2) and

$$(3) \quad E_{h/2} = c \frac{h^q}{2^q} + O(h^{q+1}).$$

The order of convergence q can be estimated as follows

$$(4) \quad q \approx \log_2 \frac{E_h}{E_{h/2}}.$$

The convergence rates were estimated using both the maximum norm

$$E_{max} = \|U - p_h u\|_{max} = \max_{i=1}^M |U_{i+1/2} - u(\hat{x}_{i+1/2})|,$$

and the mean-square norm

$$E_{L_2} = \|U - p_h u\|_{L_2} = \left(\sum_{i=1}^{M-1} (U_{i+1/2} - u(\hat{x}_{i+1/2}))^2 VC_{i+1/2} \right)^{\frac{1}{2}},$$

where $U_{i+1/2}$ is the solution of the finite-difference scheme and $u(x)$ is the exact solution.

The truncation errors were computed by applying the discrete operators to a number of test functions including the sine, cosine, exponential, and polynomials for $6 \leq r \leq 9$. All of the convergence estimates agree with our theoretical analysis for grids generated using transformations and for random grids.

2D truncation error analysis.

The truncation error was numerically investigated for the test function

$$\sin(2\pi x) \sin(2\pi y)$$

with periodic boundary conditions on the unit square and the smooth periodic grid

$$X(\xi, \eta) = \xi + \varepsilon \sin(2\pi \xi) \sin(2\pi \eta)$$

$$Y(\xi, \eta) = \eta + \varepsilon \sin(2\pi \xi) \sin(2\pi \eta).$$

The grid for parameter $\varepsilon = 0.1$ is shown in figure 4.

The numerical investigations of the truncation error for these smooth grids confirm the theoretical expectation of a fourth order truncation error.

We also investigated the truncation error on a non-smooth the random grid

$$x_{i,j} = \xi_{i,j} + R_{i,j}^\xi \lambda (\Delta \xi)^k$$

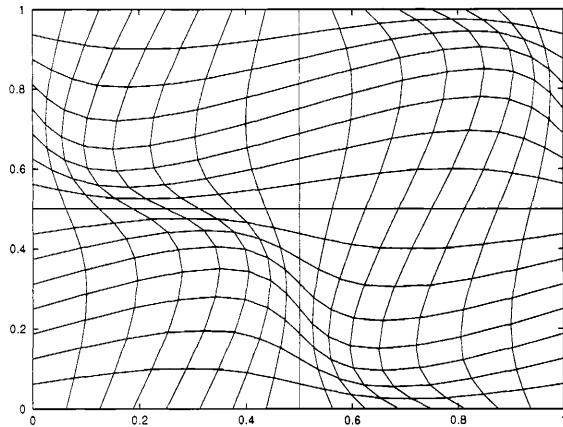


Figure 4: Smooth grid in unit square.

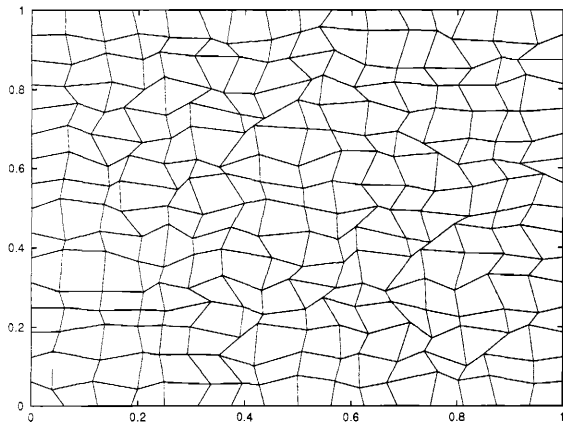


Figure 5: Random grid in unit square.

$$y_{i,j} = \eta_{i,j} + R_{i,j}^{\eta} \lambda (\Delta\eta)^k,$$

where $\Delta\xi = 1/(M-1)$, $\Delta\eta = 1/(N-1)$ are the steps in the logical grid, $R_{i,j}^{\xi}, R_{i,j}^{\eta} \in (-0.5, 0.5)$ are random numbers, k is the analog of smoothness of the grid, and λ the parameter which determined the relative size of the perturbations of the uniform grid. In figure 5 we present such a grid for $k=1$ and $\lambda=0.8$.

The numerical truncation errors for these rough random grids were different from the one dimensional results in table 1. We found no direct dependence between the order of perturbation and the order of the truncation error as we found for the one dimensional case. This implies that in 2D the order of the random perturbation is insufficient to estimate the quality of the grid. But when the perturba-

tion is $O(h^3)$ or $O(h^4)$, the results coincide with the one dimensional case.

5.2 Convergence rates for the heat equation

The time-dependent one-dimensional heat equation,

$$(5) \quad \frac{\partial u}{\partial t} = \mathbf{div grad} u = \frac{\partial^2 u}{\partial x^2}, \quad 0 < x < 2\pi,$$

with periodic boundary conditions and the exact solution

$$(6) \quad u(x, t) = e^{-t} \sin(x),$$

was solved to determine how the accuracy depends upon the smoothness of the grid. Five grids, each with M points were used; a uniform grid; a smooth periodic grid,

$$(7) \quad x_i = 2\pi(i-1)h + 0.2 \sin(2\pi(i-1)h),$$

$$i = 1, \dots, M;$$

and three random perturbations of the uniform grid,

$$x_1 = 0,$$

$$x_i = 2\pi(i-1)h + R_i 2\pi h^s, \quad i = 2, \dots, M-1,$$

$$x_M = 2\pi$$

where the $R_i; i = 2, \dots, M-1$ are random numbers, $R_i \in (-1/4, 1/4)$, and $s = 3, 2, 1$.

The spatial derivatives were approximated by the second-order and fourth-order approximations constructed in this paper. The equations were integrated in time by a variable-order, variable-time step Adams-Bashforth-Moulton method to time accuracy of 10^{-9} , so that the errors related to time-integration are negligible.

The accuracy of the solutions at $t=1$ are displayed in Tables 2 and 3. The type of the grid is in the first column; the number of grid points, M , is in the second column; the next two columns give the maximum and mean-square error norms; and the estimated orders of convergence are in the next two columns. Note that the order of convergence for the maximum and mean-square norms are the same.

The second-order method has a second-order convergence rate for all grids and the fourth-order method has at least a second-order convergence for all grids. However, as the smoothness of the grid increases, so does the order of convergence for the fourth-order method.

We also conducted numerical experiments for the 2D heat equation on the presented grids with exact solution

$$u(x, t) = e^{-8\pi^2 t} \sin(2\pi x) \sin(2\pi y).$$

Type of grid	M	max norm	L_2 -norm	q_{max}	q_2
Uniform grid	17	4.17E-03	7.43E-03	1.90	1.91
	33	1.11E-03	1.96E-03	1.95	1.96
	65	2.86E-04	5.06E-04	-	-
Smooth grid	17	4.78E-03	8.06E-03	1.90	1.92
	33	1.28E-03	2.12E-03	1.95	1.94
	65	3.29E-04	5.51E-04	-	-
Random grid $O(h^3)$	17	4.61E-03	7.45E-03	2.02	1.91
	33	1.13E-03	1.96E-03	1.97	1.96
	65	2.87E-04	5.06E-04	-	-
Random grid $O(h^2)$	17	5.73E-03	7.83E-03	2.14	1.97
	33	1.30E-03	1.99E-03	2.10	1.97
	65	3.03E-04	5.08E-04	-	-
Random grid $O(h)$	17	9.36E-03	1.02E-02	1.96	1.91
	33	2.40E-03	2.71E-03	2.38	2.23
	65	4.61E-04	5.75E-04	-	-

Table 2: Convergence Analysis for Second-Order Scheme. The convergence rates using the maximum, q_{max} , and L_2 norm, q_2 are computed on the series of grids with $M = 17, 33$, and 65 points.

Type of grid	M	max norm	L_2 -norm	q_{max}	q_2
Uniform grid	17	6.31E-05	1.12E-04	3.80	3.80
	33	4.52E-06	8.02E-06	3.90	3.91
	65	3.01E-07	5.32E-07	-	-
Smooth grid	17	1.53E-04	2.24E-04	3.75	3.79
	33	1.13E-05	1.62E-05	3.88	3.91
	65	7.66E-07	1.07E-06	-	-
Random grid $O(h^3)$	17	5.26E-04	5.04E-04	3.91	3.81
	33	3.49E-05	3.59E-05	4.32	4.31
	65	1.74E-06	1.80E-06	-	-
Random grid $O(h^2)$	17	1.41E-03	1.14E-03	3.04	2.64
	33	1.71E-04	1.83E-04	3.40	3.36
	65	1.61E-05	1.77E-05	-	-
Random grid $O(h)$	17	4.46E-03	4.02E-03	2.04	1.87
	33	1.08E-03	1.09E-03	2.73	2.47
	65	1.62E-04	1.96E-04	-	-

Table 3: Convergence Analysis for Fourth-Order Scheme. The convergence rates using the maximum, q_{max} , and L_2 norm, q_2 are computed on the series of grids with $M = 17, 33$, and 65 points.

The numerical results show dependence of the error in 2D on the quality of the grid similar to 1D case. That is for smooth grids we have a fourth order convergence rate, and for random grids the convergence rate decreases from 4 to 2 when we decrease the “smoothness” of the random grid - s , from four to one. It is important to note, that the worst convergence rate we encountered was $O(h^2)$, even then truncation error is $O(1)$. This fact is closely related to the nature of the heat equation and can be explained from a theoretical point of view similar to that in [11].

5.3 Efficiency of the second- and fourth-order methods

When using these approximations to solve systems of partial differential equations, often the cost of applying the discrete operator is small compared with the cost of evaluating the function that is to be operated on. For example, in a fluid dynamics calculation where the equation-of-state is evaluated by a table lookup, it may cost up to thirty arithmetic operations to evaluate the pressure at a mesh point. The five extra arithmetic operators for the fourth-order method compared to the second-order method is small compared to the large gain in accuracy. The real gain comes from requiring fewer mesh points in a calculation that has the same accuracy.

Also, when solving time dependent equations with explicit method, the stability restriction for the time step is a function of the mesh spacing. For the heat equation, the stability bound depends approximately upon $1/\min(\Delta x)^2$. Thus, if the time step is limited by the stability, rather than accuracy, the fewer mesh points required by the fourth-order method allows much larger time steps for the same accuracy.

The fourth-order approximation of the Laplacian requires 2.6 times as many arithmetic operations as the second-order approximation (13 arithmetic operations for fourth-order versus 5 for the second-order method). We compared the two methods in solving the previous example by using $M = 16$ cells for the fourth-order method and $2.6M = 42$ cells for the second-order method. The results in Table 4 for the max and L_2 norm errors demonstrate that the fourth-order method is significantly more accurate than the second-order method on smooth grids. On rough grids, the fourth-order method is only slightly worse, even with far fewer mesh points. These results agree with similar comparisons of finite difference and finite volume methods on nonuniform grids [9].

From this example, we conclude that for grids with varying degrees of smoothness, the fourth-order method is generally more efficient than the second-order method.

Type of grid	M	Order	max-norm	L_2 -norm
Uniform	42	2	6.54E-4	1.15E-3
	16	4	6.31E-5	1.12E-4
Smooth	42	2	7.54E-4	1.05E-3
	16	4	1.53E-4	2.24E-4
Random grid $O(h^4)$	42	2	6.54E-4	1.15E-3
	16	4	2.28E-4	2.12E-4
Random grid $O(h^3)$	42	2	6.57E-4	1.15E-3
	16	4	5.26E-4	5.04E-4
Random grid $O(h^2)$	42	2	7.41E-4	1.16E-3
	16	4	1.41E-3	1.14E-3
Random grid $O(h)$	42	2	1.43E-3	1.53E-3
	16	4	4.46E-3	4.02E-3

Table 4: Comparison of accuracy of second- and fourth-order methods for the 1D heat equation.

6 Conclusions

We combined the support-operators method with mapping, to derive new mimetic fourth-order accurate discretizations of the divergence, gradient, and Laplacian on nonuniform grids. The discrete divergence is the negative of the adjoint of the discrete gradient and consequently the Laplacian is symmetric and negative. We verified our analytical estimates of the truncation errors by computational experiments on both smooth and rough grids. The methods displayed fourth-order truncation errors on smooth grids, and this accuracy degraded gradually as the smoothness of the grid degenerated.

A numerical investigation of the order of convergence for the heat equation verified that the fourth-order method converges to at least second-order in even the roughest grids, and the order of convergence increases from 2 to 4 as the smoothness of the grid increases. Moreover, the fourth-order method was significantly more accurate than the second-order method when both methods used the same computational effort.

Acknowledgments

We thank Blair Swartz for many helpful and simulating discussions.

This work performed under the auspices of the US Department of Energy under contract W-7405-ENG-36 and the DOE/BES Program in the Applied Mathematical Sciences contract KC-07-01-01.

References

- [1] J.E. Castillo and M.J. Shashkov, *Grid Generation Methods Consistent with Finite-Difference Schemes*, LA-UR-93-2932, Los Alamos National Laboratory, Los Alamos, NM, 1993.
- [2] J.E.Castillo, J.M.Hyman, M.J.Shashkov and S.Steinberg, *The Sensitivity and Accuracy of Fourth Order Finite-Difference Schemes on Nonuniform Grids in One Dimension*, Computers Math. Applic., Vol. 30, No. 8, pp. 41-55, 1995.
- [3] J.C. Ferreri and M.A. Ventura, *On the Accuracy of Boundary Fitted Finite-Difference Calculations*, International Journal for Numerical Methods in Fluids, **4** (1984), 359-375.
- [4] B.Fornberg and D.M.Sloan, *A Review of Pseudospectral Methods for Solving Partial Differential Equations*, Acta Numerica, Cambridge University Press, (1994), pp.203-263.
- [5] R.G. Hindman, *Generalized Coordinate Forms of Governing Fluid Equations and Associated Geometrically Induced Errors*, AIAA J., **20** (1982), 1359.
- [6] J.D. Hoffman, *Relationship Between the Truncation Errors of Centered Finite-Difference Approximations on Uniform and Nonuniform Meshes*, J. Comput. Phys., **46** (1982), 469-474.
- [7] J.M. Hyman and B. Larrouturou, *The Numerical Differentiation of Discrete Functions Using Polynomial Interpolation Methods*, Appl. Math. and Comp., **10-11** (1982), 487-506.
- [8] J.M. Hyman, *Accurate Monotonicity Preserving Cubic Interpolation* SIAM J. Sci. Stat. Comput., **4** (1983), 645-654.
- [9] J.M. Hyman, R.J. Knapp and J.C. Scovel, *High Order Finite Volume Approximation of Differential Operators on Nonuniform Grids*, Physica **D**, **60** (1992), 112-138.
- [10] P. Knupp, and S. Steinberg, *Fundamentals of Grid Generation* CRC Press, Boca Raton, 1993.
- [11] H.-O. Kreiss, T.Manteuffel, B.Swartz, B.Wendroff and A.White, *Supra-Convergent Schemes on Irregular Grids*, Math. Comput. **47**, (1986), pp.537-554.
- [12] D. Lee and Y.M. Tsuei, *A Formulae for Estimation of Truncation Error of Convection Terms in a*

- Curvilinear Coordinate System*, J. Comput. Phys., **98** (1992), 90-100.
- [13] S.K. Lele, *Compact Finite Difference Schemes with Spectral-like resolution*, J. Comput. Phys., (1992), **103**, pp.16-42.
- [14] R.W. MacCormac and A.J. Paullay, *The Influence of the Computational Mesh on Accuracy for Initial Value Problems with Discontinuous or Non-Unique Solutions*, Computers & Fluids, **2** (1974), 339-361.
- [15] C.W. Mastin, *Error Analysis and Difference Equations on Curvilinear Coordinate Systems*, Large Scale Scientific Computation, Proceeding of a Conference Conducted by the Mathematical Research Center, The University of Wisconsin-Madison, May 17-19, 1983, Edited by S.V. Parter, Academic Press, Inc., 1984, pp. 195-214.
- [16] C.W. Mastin and J.F. Thompson, *Errors in Finite-Difference Computations on Curvilinear Coordinate Systems*, Mississippi State University, Engineering & Industrial Research Station, MSSU-EIRS-ASE-80-4, 1980.
- [17] E.K. de Rivas, *On the Use of Nonuniform Grids in Finite-Difference Equations*, Journal of Computational Physics, **10** (1972), 202-210.
- [18] A.A. Samarskii, V.F. Tishkin, A.P. Favorskii, and M.Yu. Shashkov, *Operational Finite-Difference Schemes*, Diff. Eqns., **17** (1981), 863-885.
- [19] M. Shashkov and S. Steinberg, *Support-Operator Finite-Difference Algorithms for General Elliptic Problems*, J. Comput. Phys., **118**, 131-151, (1995).
- [20] J.F. Thompson, Z.U.A. Warsi, and C.W. Mastin, *Numerical Grid Generation: Foundations and Applications*, North-Holland, Elsevier, New York, 1985.
- [21] H.H. Wong and G.D. Raithby, *Improved Finite-Difference Methods Based on a Critical Evaluation of the Approximation Errors*, Numerical Heat Transfer, **2** (1979), pp. 139-163.

